

# Generation of Superposition States and Charge-Qubit Relaxation Probing in a Circuit

O. P. de Sá Neto,<sup>1,\*</sup> M. C. de Oliveira,<sup>1,†</sup> and A. O. Caldeira<sup>1</sup>

<sup>1</sup>*Instituto de Física Gleb Wataghin, Universidade Estadual de Campinas,  
P.O. Box 6165, CEP 13083-970, Campinas, São Paulo, Brazil*

(Dated: March 10, 2022)

We demonstrate how a superposition of coherent states can be generated for a microwave field inside a coplanar transmission line coupled to a single superconducting charge qubit, with the addition of a single classical magnetic pulse for chirping of the qubit transition frequency. We show how the qubit dephasing induces decoherence on the field superposition state, and how it can be probed by the qubit charge detection. The character of the charge qubit relaxation process itself is imprinted in the field state decoherence profile.

PACS numbers: 03.65.Yz, 03.65.Ud

## I. INTRODUCTION

Generation of non-classical states of the electromagnetic field has been one of the most pursued problems in quantum optics [1]. This interest was reinforced in the last years due to its potential applicability in quantum information [2]. Aside from the experimental effort to generate single photon states, the generation of superposition of coherent states has been for a long time a central task, with some successful attempts. Superposition of coherent states, commonly known as Schrödinger cat states, were firstly generated in a superconducting microwave cavity field interacting with flying Rydberg atoms and its decoherence time was measured in [3] also employing Rydberg atoms sequentially interacting with the field following a previous theoretical proposal [4]. More recently these states were generated in a propagating field by photon-subtraction from a Gaussian state [5]. Indeed, special superpositions, known as odd and even coherent states have well defined parities and can have immediate application to encode quantum bits in a robust way [6]. In the last few years a new technology for coupling superconducting qubits to coplanar waveguides has been developed to an outstanding level [7]. Many different tests have been developed and interesting quantum optical experiments have been implemented in superconducting circuits [8]. Then, a simple question could be posed on how to generate a superposition of coherent states in this kind of system, and subsequently how to probe its decoherence due to dissipative effects of the qubit or the field. To our knowledge the only proposals in that direction employ a SQUID-type two-level system coupled to a microwave field [9], and a micromechanical resonator coupled to a Cooper-Pair Box [10] (See Ref. [9] for a complete list of connected proposals in distinct technologies). However none of those proposals bear a resemblance with the neat experiment in [3].

In this paper we show how to proceed to generate a

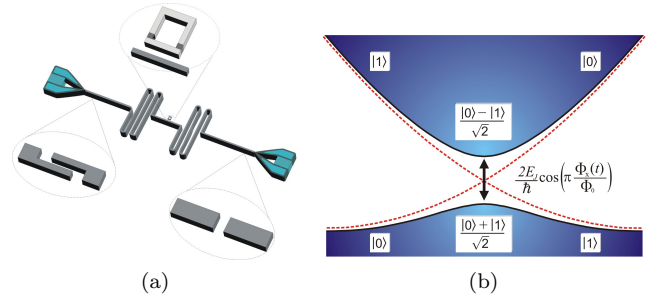


FIG. 1. (a) Schematic setup, with the central transmission line (resonator) capacitively coupled to the source and drain, and capacitively coupled to a SQUID-type qubit. (b) Variable energy levels of the qubit ( $0 < n_g < 1$ ), with an external classical magnetic flux  $\Phi_x(t)$ . The resonator field is always blue detuned from that transition.

superposition of coherent states of a microwave field in a transmission line resonator through the interaction with a single superconducting charge qubit controlled by an external single classical magnetic pulse. In contrast to the proposal in Ref. [9], which employs of a switchable interaction between the qubit and the microwave field, we assume a continuously varying magnetic pulse, and show how the generation can be almost deterministic in that way. The present proposal has the advantage to resemble the experiment in [3] in a realistic ground, allowing thus for decoherence probing through sequential qubit measurements and sequential classical magnetic pulses. We show that the qubit states dephasing is the most relevant dissipative effect leading to decoherence of preselected field states. Employing actual experimental parameters we show that this proposal is compatible with present technology, and could be actually implemented.

## II. TIME DEPENDENT FIELD-QUBIT COUPLING

Cavity quantum electrodynamics in superconducting circuits offer a exquisite playground for quantum infor-

\* opsn@ifi.unicamp.br

† marcos@ifi.unicamp.br

mation processing, and has provided the first coherent coupling between an ‘‘artificial atom’’, the charge qubit, and a field mode of a resonator [7, 11]. Mappings of qubit states [12], and also tests for fundamental problems, such as the Purcell effect [12] and photon number state resolving [13] have also been achieved. The setup employed in all those remarkable experiments is shown in Fig. 1a, where a niobium transmission line resonator is capacitively coupled to a source (on the left) and to a drain (on the right). The resonator is also capacitively coupled to the charge states of a SQUID [14]. The advantage of employing a SQUID is that the charge states can be addressed and manipulated in such a way to be set close or far from resonance with a given resonator field mode by an externally applied classical magnetic flux. By considering only the ground and the first excited states near the charge degeneracy point, the superconducting device can be well approximated by a two level system (Fig. 1b), here addressed as a qubit. In this regime the Hamiltonian [11] describing a quantized electromagnetic field mode coupled to the charge qubit is given by

$$H = \hbar\omega a^\dagger a + H_S \quad (1)$$

where

$$H_S = -\frac{1}{2}B_z\sigma_z - \frac{1}{2}B_x\sigma_x, \quad (2)$$

is the Hamiltonian for the qubit-field joint system, where  $B_z \equiv 4E_C(1-2n_g)$ , being  $E_C \equiv e^2/2(C_g+C_j) = e^2/2C_\Sigma$ , the single electron charging energy with  $C_g$  as the gate capacitance (associated to the accumulated charge in the island capacitively coupled to the central transmission line resonator) and  $C_j$  the Josephson capacitance, respectively.  $n_g \equiv C_g V_g(t)/2e$  and at the center of the transmission line resonator the voltage is given by  $V_g(t) = \sqrt{\frac{\hbar\omega}{Lc}}(a^\dagger + a)$ , where  $L$  is the length and  $c$  is the capacitance density of the transmission line. Here,  $a$  ( $a^\dagger$ ) is the usual annihilation (creation) operator for the resonator field second mode of frequency  $\omega$ ,  $\sigma_x = |0\rangle\langle 1| + |1\rangle\langle 0|$  and  $\sigma_z = |0\rangle\langle 0| - |1\rangle\langle 1|$ , involving the ground,  $|0\rangle$ , and first excited,  $|1\rangle$ , charge states of the superconducting device.  $B_x \equiv 2E_J \cos\left[\pi \frac{\Phi_x(t)}{\Phi_0}\right]$ , is the Cooper-pair tunneling energy for two Josephson junctions,  $\Phi_0 = hc/2e$  is the quantum of magnetic flux,  $\Phi_x(t)$  is a time dependent classical magnetic flux externally applied to the SQUID. All other quantities are typical constants characteristic of the device [14]. Collecting all terms the Hamiltonian, Eq. (1) reads

$$H = \hbar\omega a^\dagger a + E_J \cos\left[\pi \frac{\Phi_x(t)}{\Phi_0}\right] \sigma_x + \hbar g \sigma_z (a^\dagger + a) \quad (3)$$

being  $g = (eC_g/C_\Sigma)\sqrt{\hbar\omega/Lc}$  the coupling between the ‘‘artificial atom’’ (qubit) and the resonator mode. In Eq. (3) we neglected, as usual, the term  $-(e^2/C_\Sigma)\sigma_z$  corresponding to a DC voltage shift.

When the atomic Hamiltonian is diagonalized, the first two energy levels as a function of the gate charge

$n_g \equiv C_g V_g/2e$  are described in fig. 1b, where the vertical axis represents the energy and the horizontal represents the gate charge which is limited by the gate voltage. Changing the basis through a rotation,  $\sigma_z \rightarrow \sigma_x$  and  $\sigma_x \rightarrow -\sigma_z$ , and going to the rotating frame with the field frequency,  $\omega$ , through  $R_f = \exp[i\omega t(\sigma_z + a^\dagger a)]$ , gives

$$\begin{aligned} R_{af} H R_{af}^\dagger \underbrace{R_{af} |\psi\rangle}_{|\psi'\rangle} &= i\hbar R_{af} \frac{\partial}{\partial t} R_{af}^\dagger \underbrace{R_{af} |\psi\rangle}_{|\psi'\rangle} \\ &= i\hbar R_{af} \left( \frac{\partial}{\partial t} R_{af}^\dagger \right) |\psi'\rangle \\ &\quad + i\hbar R_{af} R_{af}^\dagger \left( \frac{\partial}{\partial t} |\psi'\rangle \right) \end{aligned}$$

resulting in

$$\underbrace{\left\{ R_{af} H R_{af}^\dagger - i\hbar R_{af} \left( \frac{\partial}{\partial t} R_{af}^\dagger \right) \right\}}_{H'} |\psi'\rangle = i\hbar \frac{\partial}{\partial t} |\psi'\rangle$$

with the transformed Hamiltonian given by

$$H' = \sigma_z \left( E_J \cos\left[\pi \frac{\Phi_x(t)}{\Phi_0}\right] - \hbar\omega \right) + \hbar g \tilde{\sigma}_x (\tilde{a}^\dagger + \tilde{a}) \quad (4)$$

where  $\tilde{\sigma}_x = \sigma_+ \exp(2i\omega t) + \sigma_- \exp(-2i\omega t)$ ,  $\tilde{a} = a \exp(-i\omega t)$  and  $\tilde{a}^\dagger = a^\dagger \exp(i\omega t)$ , with  $\sigma_x = |- \rangle \langle + | + | + \rangle \langle - |$  and  $\sigma_z = |- \rangle \langle - | - | + \rangle \langle + |$ . This new Hamiltonian (4), is analogous to the usual one for atom-field dipole interaction. The appropriate experimental regime is  $\hbar g \ll \left( E_J \cos\left[\pi \frac{\Phi_x(t)}{\Phi_0}\right] - \hbar\omega \right) \ll \Delta$ , where  $\Delta$  is the superconducting energy gap. In the following we shall consider a specific time dependent external classical magnetic pulse  $\Phi_x(t)$  applied to the SQUID, in order to bring the two lower states closer to resonance with the resonator field. As we will show, during the pulse, the field accumulates a phase conditioned to the qubit state. For that we consider the resonator field as being always far blue-detuned from these two lower atomic states, and so we must keep the counter-rotating terms [13]. With that in mind we derive the formal solution for the evolution operator

$$\begin{aligned} U(t, t_0) &= 1 + \sum_{n=1}^{\infty} \frac{1}{(i\hbar)^n} \int_{t_0}^t dt_1 \int_{t_0}^{t_1} dt_2 \dots \int_{t_0}^{t_{n-1}} dt_n \\ &\quad \times \tilde{V}^I(t_1) \tilde{V}^I(t_2) \dots \tilde{V}^I(t_n), \end{aligned} \quad (5)$$

with  $\tilde{V}^I(t) \equiv U_0^\dagger \{g\tilde{\sigma}_x (\tilde{a}^\dagger + \tilde{a})\} U_0$ , and

$$U_0 = \exp\left[ i\sigma_z \int_{t_0}^t dt' \left( \frac{E_J}{\hbar} \cos\left[\pi \Phi_x(t')/\Phi_0\right] - \omega \right) \right].$$

For  $k_B T \ll E_J \ll E_C \ll \Delta$ , a perturbative approach up to second order in  $g$  in Eq. (5) is sufficient to describe the dynamics of the system. For that the temperature must be as low as 30mK, which is consistent with this kind of experiment. In what follows

we consider the solution of (5) through time-dependent perturbation with  $H_0 = \sigma_z \left( E_J \cos \left[ \pi \frac{\Phi_x(t)}{\Phi_0} \right] - \hbar\omega \right)$  and  $V_I^S = \hbar g (\tilde{\sigma}^+ + \tilde{\sigma}^-) (\tilde{a}^\dagger + \tilde{a})$ , with  $H_0 \gg V_I^S$ , since we are interested in the radiation field blue detuned from the qubit transition, which on its turn oscillates with time. For our numerical calculations, we use the following classical magnetic flux

$$\Phi_x(t) = \frac{A\Phi_0}{2} \cos[\sigma t + \varphi], \quad (6)$$

where  $A = 0.7$  is a strength constant, and  $\sigma = 8\pi \times 10^6 \text{Hz}$  is the frequency of the classic magnetic pulse applied to the qubit in accordance with experimental values. By further assuming typical experimental parameters to reach  $k_B T \ll E_J \ll E_C \ll \Delta$ , for  $T \approx 30 \text{mK}$ , we set  $k_B T \approx 3 \mu\text{eV}$ ,  $E_J/\hbar \approx 15,9 \times 10^{10} \text{Hz}$ ,  $E_C = 250 \mu\text{eV}$  and  $\Delta \approx 458,3 \mu\text{eV}$ . The frequency of the field in the resonator,  $\omega = 90 \times 10^{10} \text{Hz}$ , is also compatible with the experiments, for which the resonator quality factor  $Q = \frac{\epsilon}{\delta\omega} \rightarrow 10^4 - 10^6$  is achievable [15].

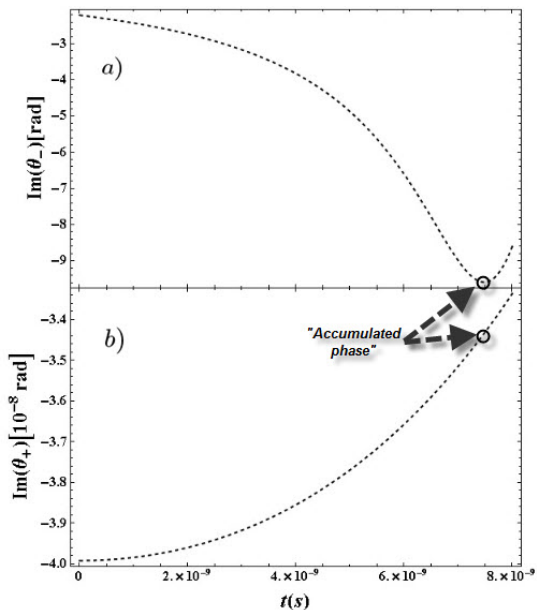


FIG. 2. Phase of the resonator coherent field, due to the time dependent interaction with the qubit prepared in *a*) the ground state, and *b*) the excited state. The pulse  $\Phi_x(t)$  oscillates for a half period ( $\Delta t \approx 7.5 \text{ns}$ ) with frequency  $8\pi \times 10^6 \text{Hz}$ .

### III. ACCUMULATED PHASE AND CONDITIONAL GENERATION OF SUPERPOSITION STATES

In order to depict our results in a more convenient way we choose that the field in the central line resonator is prepared in a coherent state  $|\alpha\rangle$  with an average number of photons smaller than one, so that we can make the

following approximation for short time,  $1 + \theta_\pm(t)a^\dagger a \approx e^{[\theta_\pm(t)a^\dagger a]}$  (see the Appendix) so that

$$[1 + \theta_\pm(t)a^\dagger a] |\pm\rangle |\alpha\rangle \rightarrow e^{-\frac{1}{2}|\alpha|^2 f_\pm(t)} |\pm\rangle \left| \alpha e^{\theta_\pm(t)} \right\rangle \quad (7)$$

where  $f_\pm(t) = [1 - e^{2\text{Re}(\theta_\pm(t))}]$ ,  $\theta_\pm(t) = 1 + \frac{F_\pm(t)}{G_\pm(t)}$ , being

$$F_\pm(t) = \int_0^t dt_1 e^{\mp 2i \left( \int_0^{t_1} dt' \Omega(t') \right) \mp i\omega t_1} \times \int_0^{t_1} dt_2 e^{\pm 2i \left( \int_0^{t_2} dt'' \Omega(t'') \right) \pm i\omega t_2}, \quad (8)$$

$$G_\pm(t) = \int_0^t dt_1 e^{\mp 2i \left( \int_0^{t_1} dt' \Omega(t') \right) \pm i\omega t_1} \times \int_0^{t_1} dt_2 e^{\pm 2i \left( \int_0^{t_2} dt'' \Omega(t'') \right) \mp i\omega t_2}, \quad (9)$$

with  $\Omega(t) = \omega - \frac{E_J}{\hbar} \cos \left[ \pi \frac{\Phi_x(t)}{\Phi_0} \right]$ , as given by the second order terms from Eq. (5). From Eq. (7) it is possible to understand that as the qubit is brought closer to resonance with the resonator field, it will imprint an accumulated phase on it, given by  $\text{Im}[\theta_\pm(t)]$  conditioned on the qubit state  $|\pm\rangle$ . In Fig. 2 we depict the numerical results for those two conditioned accumulated phases. We see that practically only when the qubit is in the state  $|-\rangle$  the phase in  $\alpha$  is changed. With an appropriate accumulation of  $-3\pi$ , as shown in Fig. 2a, it is possible to create a state  $|-\alpha\rangle$  if the qubit is initially in the  $|-\rangle$  state. We have consistently checked that this approximation is indeed very good, not only for small  $\alpha$ , if we respect a balance between the field intensity and the operation time. Moreover, we observed that around the time of optimal phase accumulation,  $t_{op} = 7.5 \text{ns}$ , the real part of  $\theta_\pm(t)$ , related to damping or amplification, is negligible, ( $\approx 10^{-3} - 10^{-4}$ ), so that in Eq. (7),  $f_\pm(t) = 0$  at the instant of measurement as shown in the Appendix, and shall not be considered from now on.

To generate the superposition of coherent states for the field, we note that due to the low temperature of the system it is easy to prepare the qubit state initially in  $|0\rangle$ . Obviously the decoupled coherent state of the resonator and the qubit state may be written as  $|0\rangle \otimes |\alpha\rangle = (|-\rangle + |+\rangle) \otimes |\alpha\rangle / \sqrt{2}$ . If the aforementioned pulse is applied to the qubit, coupling it to the resonator field through the evolution given by Eq. (5), we shall have

$$U(t_0 + \Delta t, t_0) |0\rangle \otimes |\alpha\rangle \xrightarrow{\text{Pulse}} \frac{|-\rangle \otimes |-\alpha\rangle + |+\rangle \otimes |\alpha\rangle}{\sqrt{2}}, \quad (10)$$

or  $[|0\rangle \otimes (|-\alpha\rangle + |\alpha\rangle) + |1\rangle \otimes (|-\alpha\rangle - |\alpha\rangle)]/2$ , which is an entangled state between the qubit and the resonator field. Consequently, the resonator field can be left in an odd or even superposition of coherent states depending on the detection of the qubit state with a single electron transistor [14].

#### IV. FIELD STATE DECOHERENCE AND QUBIT RELAXATION PROBING

Certainly, the exact preparation of such a state is compromised by external noise. In contrast to experiments with microwave fields and Rydberg atoms, dissipative effects are most noticeable for the qubit states, which can flip from the ground state to the excited one and vice versa due to thermal effects and inductive coupling of the qubit to the external circuit. While the relaxation time of the qubits are of the order of  $10^{-6}$ s, the relaxation of the resonator field is of the order of  $10^{-3}$ s and can, in principle, be neglected. If compared with the time of the pulses for the accumulated phase of the field,  $\Delta t \approx 7.5 \times 10^{-9}$ s, the relaxation of the atom is negligible as well, but certainly will be important if any further manipulation is to be executed. So in fact the effects of dissipation are more relevant after the pulse is applied, i.e., when  $\Phi_x(t) = 0$ , and will affect the probability to detect a given qubit state, and consequently the generation of an appropriate field. To understand the effects of noise in the system, we couple the qubit two-state to a bath of harmonic oscillators in an adaptation of the standard spin-boson model with Ohmic dissipation [14, 17, 18], through the Hamiltonian  $H = H_S + H_{AR} + H_R$ . Here  $H_S$  is given by Eq. (2), presented in reference [14], with the convention at the degeneracy point  $|+\rangle = (|0\rangle - |1\rangle)/\sqrt{2}$ , and  $|-\rangle = (|0\rangle + |1\rangle)/\sqrt{2}$ . Eq. (2) can be conveniently rewritten as

$$H_S = -\frac{\Delta E}{2} \left( \frac{1}{\sqrt{2}} \sigma_z + \frac{1}{\sqrt{2}} \sigma_x \right), \quad (11)$$

where  $\Delta E = \sqrt{B_z^2 + B_x^2}$ , and now since  $\Phi_x(t) = 0$ ,  $B_z \equiv 4E_C(1 - 2n_g)$ , and  $B_x \equiv 2E_J$ . Thus  $\Delta E = \sqrt{(2E_J)^2 + 16E_C^2(1 - 2n_g)^2}$ , and conveniently choosing  $n_g = 0.5$  we end up with  $\Delta E = 2E_J$ . The coupling of the qubit to the bath is given by

$$H_{AR} = \sigma_z \sum_a \lambda_a x_a, \quad (12)$$

and

$$H_R = \sum_a \left( \frac{p_a^2}{2m_a} + \frac{m_a \omega_a^2 x_a^2}{2} \right), \quad (13)$$

corresponds to the bath free Hamiltonian.

The master equation for the evolution of the two level system coupled to a bath in a thermal state  $\rho_R = \exp[H_R/k_B T]$  was extensively studied in the past [17, 18]. We employ solutions corresponding to an Ohmic bath [14, 17, 18]. By taking the previous initial state,  $|0\rangle|\alpha\rangle$ , the main consequence of the qubit relaxation will be on the probability to generate the superposition states  $|0\rangle_L = (|\alpha\rangle + |-\alpha\rangle)/\sqrt{2}$ , or  $|1\rangle_L = (|-\alpha\rangle - |\alpha\rangle)/\sqrt{2}$  after the pulse is applied. To turn our description clearer we consider the optimal time for phase accumulation as our time origin. Remark that since the central transmission line resonator field is now far detuned from the

qubit, they remain uncoupled. The only possible correlation between the qubit and the field is due to their past interaction. Taking the result for the density operator evolution from Refs. [14, 17, 18] we obtain the following joint qubit-field state

$$\rho(t) = P_0(t)|0\rangle\langle 0| \otimes |0\rangle\langle 0|_L + P_1(t)|1\rangle\langle 1| \otimes |1\rangle\langle 1|_L \quad (14) \\ + P_T(t)|1\rangle\langle 0| \otimes |1\rangle\langle 0|_L + P_T^*(t)|0\rangle\langle 1| \otimes |0\rangle\langle 1|_L,$$

where  $P_{(1)}(t) = Tr\{|(1)\rangle\langle (1)|\rho(t)\}$  is the probability to detect the qubit in the state  $|1\rangle$ , given by

$$P_{(1)}(t) = \frac{1}{2} \{ \tanh(\Lambda) + [1 - \tanh(\Lambda)] \exp(-t/\tau_r) \\ \pm \cos(\Delta E t/\hbar) \exp(-t/\tau_\varphi) \}, \quad (15)$$

and  $P_T(t) = Tr\{|0\rangle\langle 1|\rho(t)\}$  is the transition amplitude, explicitly given by

$$P_T(t) = -i \sin(\Delta E t/\hbar) \exp(-t/\tau_\varphi), \quad (16)$$

where  $\Delta E = 2E_J$ ,  $\Lambda \equiv \Delta E/2k_B T$ ,  $\tau_r = [\pi\beta\Delta E \coth(\Lambda)/\hbar]^{-1}$  is the relaxation time and  $\tau_\varphi = [\tau_r^{-1}/2 + 2\pi\beta k_B T/\hbar]^{-1}$  is the dephasing time, with  $\beta \approx 0.001$  a dimensionless parameter reflecting the strength of dissipation [14]. As  $\Delta E \gg k_B T$ ,  $\tanh(\Lambda) \approx 1$ , and so

$$P_0(t) = \frac{1}{2} [1 + \cos(\Delta E t/\hbar) \exp(-t/\tau_\varphi)], \quad (17)$$

$$P_1(t) = \frac{1}{2} [1 - \cos(\Delta E t/\hbar) \exp(-t/\tau_\varphi)], \quad (18)$$

reflecting the probability to detect the qubit in the state  $|0\rangle$  or  $|1\rangle$ , respectively, at an instant  $t$  after the classical magnetic pulse. The entangled state from Eq. (14) allows a probabilistic generation of the field superposition state, as well as an indirect probe of the qubit state by the field state measurement.

As can be readily checked, if the qubit detection is made right after the pulse is applied, there is a high probability that the state  $|0\rangle_L$  will be generated, in this case thus almost deterministically. If the detection is made after a long delay time,  $t \approx 3\tau_\varphi$ , there is 50 % chance that the qubit can be detected in  $|0\rangle$  and 50 % in  $|1\rangle$  and thus that the states  $|0\rangle_L$  or  $|1\rangle_L$ , be generated, respectively. Indeed, if a second classical magnetic pulse is applied, after a qubit detection, the state generated is exactly equal to (14) and a sequential detection after a time interval  $t$ , allows the inference of those probabilities directly from the measurement, since the conditioned probability for two consecutive detections in the state  $|0\rangle$  is  $P_{0,0}(t) = P_0(t)$ , and the probability for detecting  $|0\rangle$  and then  $|1\rangle$  is  $P_{0,1}(t) = P_1(t)$ . This contrasts with the decoherence time detection in Ref. [4]. Those probabilities are depicted in Fig. 3, for  $T = 30$  mK. There we employ an artificial  $\Delta E$ , which is  $10^3$  times smaller than the real one to depict the oscillatory profile. The probability to sequentially detect  $|0\rangle$  decreases with time, as a signature of the dephasing of the qubit states and thus on the probability to generate  $|0\rangle_L$ . Then of course the probability to generate  $|0\rangle_L$  increases with time. The decaying

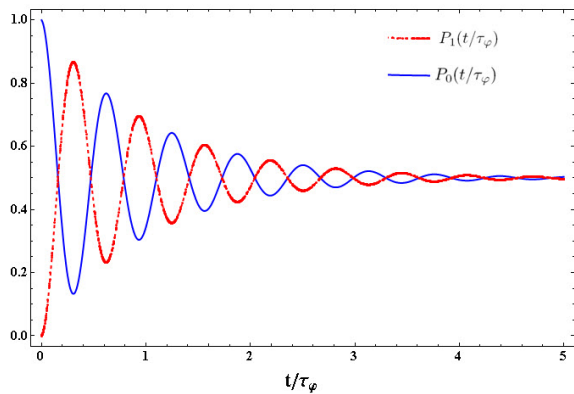


FIG. 3. Probabilities of charge qubit detections and consequently of postselected  $|0\rangle_L$ , or  $|1\rangle_L$  field states. The decoherence of the preselected field state is given by  $2P_0(t) - 1$ .

oscillatory profile depicted in Fig. 3, which represents exactly the dephasing of the qubit states, will surely be imprinted in the field states even in the absence of detections, and is a signature of the Ohmic character of the reservoir. The preselected field state derived from Eq. (14) is

$$\rho_f(t) = \frac{1}{N(t)} \left\{ |\alpha\rangle\langle\alpha| + |-\alpha\rangle\langle-\alpha| + \cos\left(\frac{\Delta E t}{\hbar}\right) e^{-t/\tau_\varphi} [|\alpha\rangle\langle-\alpha| + |-\alpha\rangle\langle\alpha|] \right\}, \quad (19)$$

with  $N(t) = 2[1 + \cos(\Delta E t/\hbar)e^{-t/\tau_\varphi}e^{-2|\alpha|^2}]$ . So, the dephasing causes the decoherence of the state  $\rho_f(t)$ , whose behavior is exactly the one depicted in fig. 3, and can be inferred as being  $2P_0(t) - 1$ . We remark that in the same sense the decoherence of the field can be used to probe different noise characters on the qubit. Here we analyzed the effect of an Ohmic bath. Would that be a super-Ohmic or sub-Ohmic its signature would be imprinted in the field decoherence.

## V. DISCUSSION

We have discussed the possibility to generate superposition states of the field due to a classical magnetic pulse which causes a chirping of the frequency of the qubit, bringing it closer to resonance with the resonator field mode. At low temperatures the dissipative effects of the field mode are almost negligible during the time interval the superposition is generated, while the dephasing of the qubit becomes the relevant source for decoherence of the state of the radiation field. In this case the qubit detection probability affects the probability for generation of the field superposition states  $|0\rangle_L$  or  $|1\rangle_L$ . Those states are quite robust against dissipation [6], and therefore may be quite relevant for quantum information processing involving a hybrid form of qubits involving field

and charge qubits. One immediate example is the Bell-like state Eq.(8), for  $t \ll \tau_\varphi$ , which may directly allow the implementation of quantum communication protocols, or indirectly through a possible coupling to other solid state qubits [16]. We leave this point for future discussion.

## ACKNOWLEDGMENTS

We thank CAPES, FAPESP, and CNPq for financial support through the National Institute for Science and Technology of Quantum Information (INCT-IQ).

## APPENDIX

In this appendix we show how Eqs. (7)-(9) are derived. For that we have to perturbatively compute how the evolution operator,  $U(t, t_0)$ , shown in Eq. (5) acts over an initial state  $|0\rangle|\alpha\rangle$ ,

$$U(t, t_0) |0\rangle|\alpha\rangle = U(t, t_0) \frac{(|-\rangle + |+\rangle)}{\sqrt{2}} |\alpha\rangle. \quad (A-1)$$

Due to the parity of the classical flux  $\Phi_x(t)$  applied over the qubit, Eq. (6), for a “fast” pulse, i.e., a pulse with duration equal to or shorter than half period of oscillations (for  $t_0 = 0$ ), the first order terms in Eq. (5) are negligible and we consider only terms of second order. So that,

$$U(t, t_0) |+\rangle|\alpha\rangle \approx -g^2 [a^\dagger a F_+(t) + a a^\dagger G_+(t)] |+\rangle|\alpha\rangle,$$

$$U(t, t_0) |-\rangle|\alpha\rangle \approx -g^2 [a a^\dagger G_-(t) + a^\dagger a F_-(t)] |-\rangle|\alpha\rangle,$$

where  $F_\pm(t)$  and  $G_\pm(t)$  are given by Eq. (8) and Eq. (9), respectively,

$$F_\pm(t) = \int_0^t dt_1 e^{\mp 2i \left( \int_0^{t_1} dt' \Omega(t') \right) \mp i \omega t_1} \times \int_0^{t_1} dt_2 e^{\pm 2i \left( \int_0^{t_2} dt'' \Omega(t'') \right) \pm i \omega t_2},$$

$$G_\pm(t) = \int_0^t dt_1 e^{\mp 2i \left( \int_0^{t_1} dt' \Omega(t') \right) \pm i \omega t_1} \times \int_0^{t_1} dt_2 e^{\pm 2i \left( \int_0^{t_2} dt'' \Omega(t'') \right) \mp i \omega t_2},$$

corresponding to terms of second order of the operator  $U(t, t_0)$  from Eq. (5).

The second member of the evolution equations above can be respectively rewritten as

$$-g^2 \{ G_+(t) + [F_+(t) + G_+(t)] a^\dagger a \} |+\rangle|\alpha\rangle,$$

$$-g^2 \{ G_-(t) + [F_-(t) + G_-(t)] a^\dagger a \} |-\rangle|\alpha\rangle,$$

or alternatively as

$$-g^2 G_+(t) \left\{ 1 + \left[ 1 + \frac{F_+(t)}{G_+(t)} \right] a^\dagger a \right\} |+\rangle|\alpha\rangle, \quad (A-2)$$

$$-g^2 G_-(t) \left\{ 1 + \left[ 1 + \frac{F_-(t)}{G_-(t)} \right] a^\dagger a \right\} |-\rangle|\alpha\rangle. \quad (A-3)$$

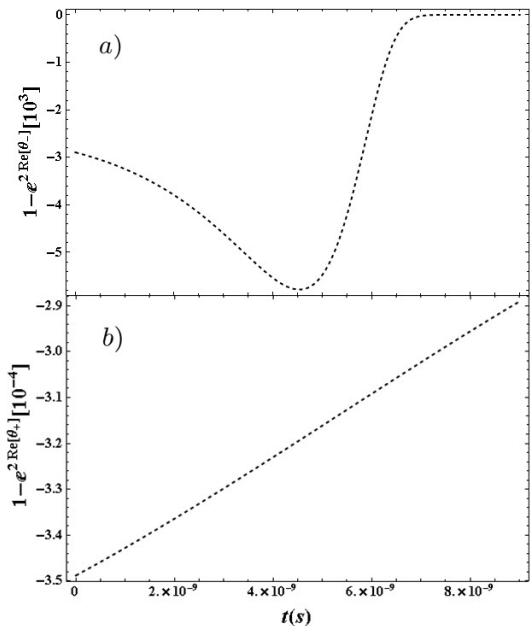


FIG. 4. The function  $f_{\pm}(t)$  operating on the states  $|\pm\rangle$ .

The terms  $-g^2G_{\pm}(t)$  give only contributions to a global phase of no implication and without any loss of generality are being neglected. For short time and small average

number of photons,  $\left[1 + \frac{F_{\pm}(t)}{G_{\pm}(t)}\right] a^{\dagger}a$  is kept small enough so that the following approximation can be employed

$$1 + \left[1 + \frac{F_{\pm}(t)}{G_{\pm}(t)}\right] a^{\dagger}a \approx \exp \left\{ \left[1 + \frac{F_{\pm}(t)}{G_{\pm}(t)}\right] a^{\dagger}a \right\},$$

and thus

$$\left[1 + \theta_{\pm}(t)a^{\dagger}a\right] |\pm\rangle |\alpha\rangle \rightarrow e^{-\frac{1}{2}|\alpha|^2 f(t)} |\pm\rangle \left| \alpha e^{\theta_{\pm}(t)} \right\rangle,$$

as in Eq. (7) where  $f_{\pm}(t) = [1 - e^{2\text{Re}\{\theta_{\pm}(t)\}}]$ ,  $\theta_{\pm}(t) = 1 + \frac{F_{\pm}(t)}{G_{\pm}(t)}$ . This approximation has to be taken with caution. As shown in Fig. (4a),  $f_{-}(t)$  increases to large (negative) values, achieving its maximal value around 4.5ns meaning that at those times the approximation in Eq.(7) is not good enough. However closer to the time of optimal phase accumulation,  $t_{op} = 7.5\text{ns}$ , in Fig. (2),  $f_{-}(t)$  decreases rapidly to  $(\approx 10^{-3} - 10^{-4})$ , meaning that the accumulated real part of the pulse is negligible well before the end of the pulse. On the other hand the function  $f_{+}(t) = 1 - e^{2\text{Re}\{\theta_{+}(t)\}}$ , shown in Fig. (4b), is always very small, of order  $10^{-3} - 10^{-4}$ , during the time of the pulse. Thus showing the validity of the approximation in Eq. (7), is consistent for the time of the pulse.

Now at the optimal time,  $t_{op}$ , since  $f_{\pm}(t_{op}) \approx 0$ , Eq. (7) can be effectively written as

$$\left[1 + \theta_{\pm}(t_{op})a^{\dagger}a\right] |\pm\rangle |\alpha\rangle \approx |\pm\rangle \left| \alpha e^{\theta_{\pm}(t_{op})} \right\rangle. \quad (\text{A-4})$$

- 
- [1] S. Haroche and J. M. Raimond, in *Cavity Quantum Electrodynamics*, edited by P. Berman (Academic Press, NY, 1994).
- [2] S. Haroche and J.M. Raimond, *Exploring the Quantum: Atoms, Cavities, and Photons*, (Oxford University Press, NY,USA, 2006).
- [3] M. Brune et al., Phys. Rev. Lett. **77**, 4887 (1996).
- [4] M. Brune, S. Haroche, J. M. Raimond, L. Davidovich and N. Zagury, Phys. Rev. A **45**, 5193 (1992); L. Davidovich, M. Brune, J. M. Raimond and S. Haroche, Phys. Rev. A **53**, 1295 (1996).
- [5] A. Ourjoumtsev, R. Tualle-Brouri, J. Laurat, and P. Grangier, Science **312**, 83 (2006).
- [6] M.C. de Oliveira and W.J. Munro, Phys. Rev. A **61**, 042309 (2000).
- [7] A. Wallraff et al., Nature **431**, 162 (2004).
- [8] S.M. Girvin, M.H. Devoret, and R.J. Schoelkopf, Phys. Scr. **T137**, 014012 (2009).
- [9] Y. Liu, L.F. Wei and F. Nori, Phys. Rev. A **71** 063820 (2005).
- [10] A.D. Armour, M.P. Blencowe, and K.C. Schwab, Phys. Rev. Lett. **88**, 148301 (2002).
- [11] A. Blais et al., Phys. Rev. A **69**, 062320 (2004).
- [12] A. A. Houck et al., Nature **449**, 328 (2007).
- [13] D. I. Schuster, A. A. Houck, J. A. Schreier, A. Wallraff, J. M. Gambetta, A. Blais, L. Frunzio, J. Majer, B. Johnson, M. H. Devoret, S. M. Girvin e R. J. Schoelkopf, Nature **445**, 515 (2007).
- [14] Y. Makhlin, G. Schon and A. Shnirman, Rev. Mod. Phys. **73**, 357 (2001).
- [15] L. Frunzio et al., IEEE Trans. Appl. Sup. **15**, 860 (2005).
- [16] L. DiCarlo et al., Nature **460**, 240 (2009).
- [17] A. J. Leggett, S. Chakravarty, A. T. Dorsey, M. P. A. Fisher, A. Garg, and W. Zwerger, Rev. Mod. Phys. **59**, 1 (1987).
- [18] U. Weiss, *Quantum Dissipative Systems*, 2nd ed. (World Scientific, Singapore, 1999).